Acta Neuropathol (2001) 101:92–100
DOI 10.1007/s004010000252

REGULAR PAPER

Kyoko Itoh · Kyoko Suzuki · Karl Bise · Hiroshi Itoh
Parviz Mehraein · Serge Weis

Apoptosis in the basal ganglia of the developing human nervous system

Received: 14 September 1999 / Revised: 21 January 2000, 14 April 2000 / Accepted: 20 April 2000 / Published online: 25 November 2000

Abstract Programmed cell death (PCD) plays a crucial role in the development of the central nervous system through controlling neuronal numbers and adequate synaptic connections. PCD has been considered to occur in the form of apoptosis. To examine how apoptosis occurs in the developing human brain, we performed a morphometric TUNEL study, using a commercially available kit (ApopTag Kit, Oncor Inc.). We examined apoptotic cells in the basal ganglia of 47 fetuses and newborns without macroscopical and microscopical evident congenital anomalies. Gestational age ranged from 12 to 40 weeks. The numerical density as well as the labeling index of TUNEL-positively labeled nuclei were evaluated. In the caudate nucleus and putamen, TUNEL-labeled cells were observed around the 12th week of gestation. The numerical density of total cells was significantly decreased, whereas the labeling index of apoptotic cells was significantly increased with advanced gestational age. In the globus pallidus, the numerical density of total cells decreased with advancing gestational age, while the labeling index of apoptotic cells increased between the 20th and 28th week, followed by a decrease until the 40th week. The analysis of TUNEL-positive cells revealed a different reaction pattern for the various basal ganglia with regard to the timing and degree of the apoptotic process in regulating cell numbers.

Keywords Apoptosis · Programmed cell death · Morphometry · Brain development · TUNEL method

S. Weis (✉)
Institute of Neuropathology, Otto-von-Guericke University, Leipziger Strasse 44, 39120 Magdeburg, Germany
e-mail: serge.weis@medizin.uni-magdeburg.de,
Tel.: +49-391-6715814, Fax: +49-391-6713300

K. Itoh · K. Bise · P. Mehraein · S. Weis
Institute of Neuropathology, Ludwig-Maximilians University, Munich, Germany

K. Itoh · H. Itoh
Department of Pathology, 1st Division, Kobe University School of Medicine, Kobe, Japan

K. Suzuki
Department of Psychiatry, Yokohama City University School of Medicine, Yokohama, Japan

Introduction

The development of the nervous system of many organisms is known to be accompanied by programmed cell death (PCD) of a large number of neurons at distinct periods of time [8, 14, 17, 19, 24, 32, 37, 39, 44, 45]. The execution of the latter plays a major role in morphogenetic, histogenetic and phylogenetic processes of normal and abnormal development [23, 32]. The loss of neurons occurs in various neuronal structures in the brains of vertebrates, including the cerebral cortex [14, 15], dentate gyrus [17], thalamus [41], cerebellum [2, 21], striatum [21], and substantia nigra [20]. However, exact knowledge of how cell death occurs in the developing human nervous system is still limited.

Clarke [7, 8] described the following three ways in which developing tissues die: naturally occurring cell death (Type 1, apoptosis), autophagic degeneration (Type 2), and non-lysosomal vesiculate degradation (Type 3). Most of PCD has been considered to occur in the form of apoptosis. The morphological characteristics of apoptosis encompass condensation and aggregates forming dense granular caps, crescents or balls of DNA. Electron microscopically, cell surface blebbing and "pinching off" of the extracellular membrane are observed forming "apoptotic bodies". The contents of the dying cell are contained within an intact extracellular membrane, thus, no inflammatory response is observed in the surrounding tissues despite the death of these cells. At the molecular level, electrophoretic analyses reveal that DNA is fragmented into nucleosomal lengths of regular size [15, 32]. The process of apoptosis is under cell-specific and inducer-specific genetic control. Variable genes expressed in the CNS are associated with apoptosis such as APO-1/FAS [29], c-fos

[40], c-myc [13], TRPM-2 [4, 23], p53 [28], and IL-1β-converting enzyme (ICE) [31]. Type 2 neuronal cell death, which is characterized by the presence of large numbers of lysosomal vesicles for the destruction of the cell without any evidence of DNA fragmentation, was observed in spinal motor neurons of the frog [12] and in dying neurons of the isthmo-optic nucleus in the chick embryo [6, 7]. Type 3 cell death, also observed in the developing nervous system, exhibits several features of necrotic cell death and may be a passive rather than an active or programmed form of cell death [34]. Type 1 and Type 3 forms of cell death have been observed to occur together in several neonatal systems including spinal motor neurons of the chick [5].

Recently, the TUNEL (terminal deoxynucleotidyl transferase-mediated biotin-16-dUTP nick-end labeling) method was established to detect apoptotic cells [30, 32]. The specific binding of terminal deoxynucleotidyl transferase (TdT) to 3'-OH ends of double- or single-stranded DNA results in a polydeoxynucleotide polymer. TdT is used to incorporate digoxigenin-deoxyribonucleotide triphosphate, forming a random heteropolymer at sites of DNA breaks. The signal is amplified by peroxidase, enabling conventional histochemical identification by light microscopy.

In the present study, we examined apoptotic cells in the basal ganglia of the human fetal CNS visualized by means of the TUNEL method and analyzed by morphometry to determine the form and rate of PCD in the development of human brain structures.

Materials and methods

Brains of human fetuses and newborns (n= 47; 28 female, 19 male) who were spontaneously aborted or died immediately after birth were examined. Following the clinical reports, pregnancy was uneventful. Gestational age (GA) ranged from 12 to 40 weeks of gestation. The investigated sample was divided into the following GA groups: 12–15 weeks (n=8), 16–19 weeks (n=9), 20–23 weeks (n=15), 24–27 weeks (n=6), 28–31 weeks (n= 2), and 32–40 weeks (n=7). Brain tissue taken within 24 h post mortem was used in the present study.

The brains were thoroughly examined and showed adequate brain development as related to GA without evident macroscopical or microscopical neuropathological anomalies. The brains were fixed in a 4% formalin solution for at least 1 week; subsequently frontal sections were made. Paraffin-embedded 5-μm-thick sections were prepared for the TUNEL method, which employed a commercially available kit (ApopTag Kit, Oncor Inc.) following the manufacturer's instructions. Briefly, deparaffinized sections were digested with proteinase K (20 mg/ml) for 15 min, and endogenous peroxidase quenched with 2.0% H_2O_2 for 5 min. The sections were incubated with TdT and a mixture of digoxigenin-labeled nucleotides for 60 min. This was followed by incubation with anti-digoxigenin-peroxidase for 30 min, and color development with H_2O_2-diaminobenzidine for 3–6 min. Then, the slides were counterstained with hemalum and coverslipped. For positive controls, specimens of thyroid tissue were provided by Oncor. In these specimens, PCD was seen in thyroid epithelium which showed typical chromatin fragmentation labeled with TUNEL. Negative controls were performed by omission of TdT enzyme from the incubation buffers.

The following brain regions were morphometrically evaluated: (1) caudate nucleus, (2) putamen, and (3) globus pallidus, at the level of thalamus and rostral hippocampus. Electron microscopical examinations, following standard protocols, of the same brain regions were performed to confirm the nature of apoptotic cells.

The morphometrical evaluation was made at a magnification of ×1,000 with careful registration of the morphological features. The number of TUNEL-labeled cells as well as the number of all cells was determined following the 'random systematic sampling' method [43]. Briefly, the first measuring field was positioned randomly within the structure of interest, the next measuring field was positioned systematically adjacent to the previous one; every second measuring field was considered, resulting in a total of five measuring fields. Further details of the morphometric methods have been described previously [43]. While counting the neurons, the rules of the unbiased grid were applied. Briefly, two lines of the measuring field were defined as forbidden lines. No neuronal profile hitting the forbidden lines or their extensions were counted. All neurons falling within the measuring field or touching the non-forbidden lines and their extensions were counted [18]. The numerical density was calculated as the number of cells per square millimeter (n/mm^2), and the labeling index (LI) expressed in percent [(no. of TUNEL-labeled cells/no. of all cells)×100] was also determined. The numerical density of "normal cells" (no. of total cells–no. of TUNEL-labeled cells) was also calculated. The evaluated data were processed on a PC Escom Pentium using the Statistical Package for the Social Sciences (SPSS). Correlation, one-way analysis of variance (ANOVA), and the non-parametric Mann-Whitney-U test were used. The interpolated curves were plotted using HARVARD Graphics.

Results

Qualitative results

Light microscopy

The cells labeled by the TUNEL method showed the following histological features: (a) round, shrunken nucleus with condensed chromatin, (b) slightly shrunken round nucleus with dense fragmented chromatin, (c) normal sized or slightly swollen nucleus with finely condensed chromatin, and (d) slightly swollen nucleus with chromatin margination and fragmentation. Some of the TUNEL-labeled cells were classified as necrotic cells; they were rarely encountered and amounted for less then 4% of all TUNEL-labeled cells. Necrotic cells showed irregularly fragmented nuclear chromatin or cell debris associated with lytic nuclear membrane or swollen cytoplasm. These cells were not considered in the present morphometric investigation.

The counted cells were undifferentiated stem cells including neuroblasts and glioblasts. Identification of neurons based on the presence of specific chromatin patterns and emerging dendrites was difficult in early GA. In the globus pallidus, large neurons could be observed during the 24th week of gestation. Large neurons in the striatum were observed around weeks 28–30 of gestation. Undifferentiated small stem cells, prevalent in the putamen and caudate nucleus of fetuses from the week 12 to week 32 of gestation were also evaluated in this study.

In the caudate nucleus, TUNEL-labeled cells were observed at around the 14th week of GA and were diffusely distributed in all areas of the nucleus with a slightly higher density in the region close to the subependymal germinal matrix. In the putamen, diffusely distributed

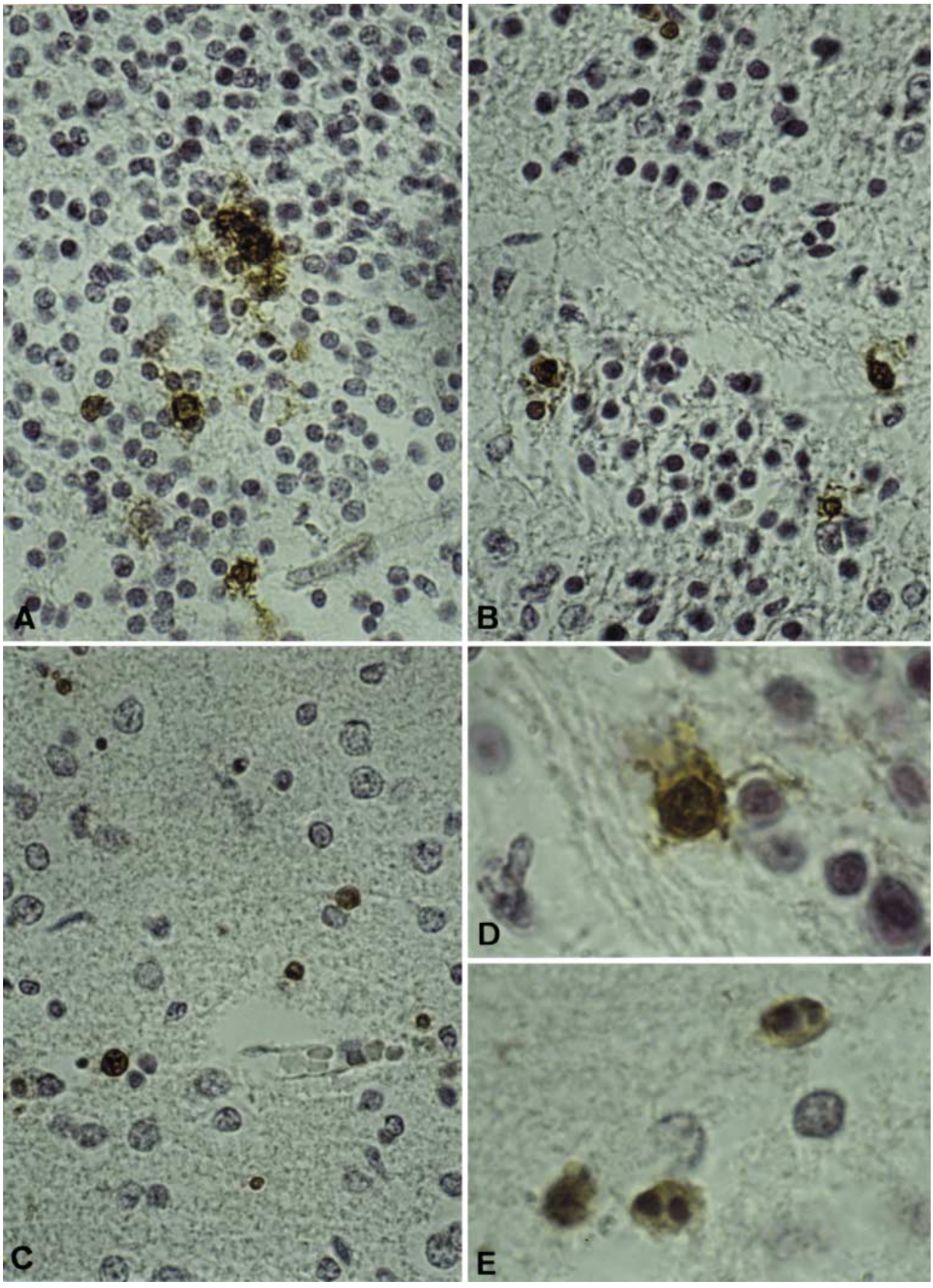

Fig. 1A–E TUNEL-labeled cells in the caudate nucleus at different gestational ages. The numerical density of total cells was decreased, whereas the density of TUNEL-labeled cells was increased with advanced gestational age. **A** Week 20 of gestation, **B** week 24 of gestation, **C** week 36 of gestation. TUNEL-labeled cells, showing various nuclear fragmentation and condensation. **D** Caudate nucleus at week 24 of gestation, and (**E**) putamen at week 36 of gestation. **A**–**C** × 400; **D**,**E** ×1,000

TUNEL-positive cells were found at the 12th week of GA. In the pontes grisei caudatolenticulares of a fetus at the 36th week of GA, TUNEL-positive cells with condensed chromatin clustered in groups of five to ten cells (Fig. 1A–D). TUNEL-labeled cells, diffusely distributed in all areas of the globus pallidus, were observed from the 18th week until the 40th week of GA.

Clustering of TUNEL-labeled cells was occasionally observed in the marginal zone of the caudate nucleus close to the subependymal germinal matrix or in the periphery of the putamen around 20–27 weeks of gestation. Clusters were also observed in the pontes grisei caudatolenticulares at the 36th week of GA. They were composed of three to four apoptotic cells with nuclear condensation or fragmentation.

Electron microscopy

Apoptotic cells showed nuclear fragmentation and condensation with a preserved nuclear membrane. Intracytoplasmic organelles were decreased, whereas some mitochondria showed normal features (Fig. 2).

Quantitative results

Descriptive statistics giving the mean, standard deviation, minimum, and maximum of the examined parameters according to the individual basal ganglia for each gestational age group are given in Table 1.

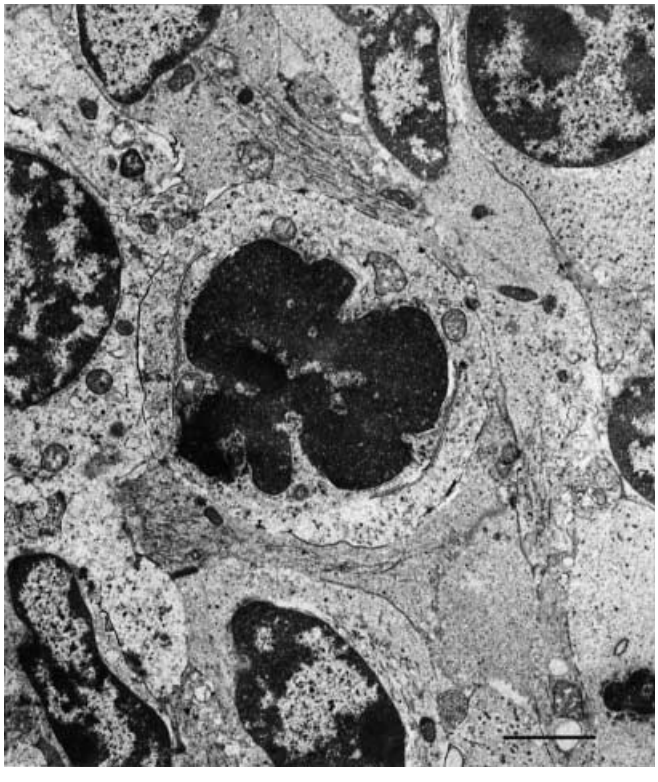

Fig. 2 Electron microscopy of an apoptotic cell showing nuclear cleavage and condensation with preserved nuclear membrane. *Bar* 2 μm

Total cells and normal cells

The numerical density of all cells as well as of normal cells was significantly decreased in the caudate nucleus, putamen with advancing gestational age (Fig. 3, Tables 1, 2). The numerical density of all cells and of normal cells was decreased in the globus pallidus with increasing gestational age; however, this difference did not reach the level of statistical significance (Fig. 3, Tables 1, 2).

TUNEL-labeled cells

The LI of TUNEL-labeled cells was significantly increased in the caudate nucleus and putamen with increased gestational age (Fig. 4, Tables 1, 2). The LI of TUNEL-labeled cells in the globus pallidus was increased between weeks 20–23 and weeks 28–31 of gestation and was decreased after week 32 until week 40 (Fig. 4, Tables 1, 2). The numerical density of apoptotic cells in the caudate nucleus was increased from week 12 to week 27 and slightly decreased until week 40 (Fig. 5, Tables 1, 2). The numerical density of apoptotic cells in the putamen was increased from gestational week 12 to week 27 and remained stable until week 40. The numerical density of apoptotic cells in the globus pallidus was increased from week 20 to weeks 28–31 of GA and was slightly decreased until week 40 (Fig. 5, Tables 1, 2).

Discussion

PCD is a selective process of physiological cell deletion in the development of multicellular organisms [35, 37]. During the development of the nervous system of vertebrates up to 50% or more of different types of neurons normally die soon after they form synaptic connections with their target cells [33, 42]. PCD occurs in neurons which have already migrated to their final destinations or occurs at about the time when their axons are forming connections [11]. The survival of developing neurons depends on several mechanisms including the retrograde transport of trophic factors such as nerve growth factor (NGF) [27]. PCD has been considered to occur in the form of apoptosis, although there are many instances in which mammalian neurons and glia undergo PCD exhibiting the morphological hallmarks of apoptosis but not satisfying all of the biochemical criteria of apoptosis in developing systems [6, 7, 8, 12].

To determine the form of PCD in the developing human fetal brain, we performed morphometrical analyses combined with the TUNEL method, which allows the detection of DNA fragmentation in apoptotic cells. In the present sample, technical problems with the TUNEL method as reported by some authors were not encountered. Following Charriaut-Marlangue and Ben-Ari [5], a

Table 1 Descriptive statistics (mean, standard deviation, minimum, and maximum) of the examined parameters according to the individual basal ganglia for each GA group (*GA* gestational age, *LI* labeling index)

	Mean	SD	Min	Max
Caudate nucleus				
GA 12–15 weeks				
Numerical density of total cells	8,288.00	2,256.36	5,013.33	10,648.89
Numerical density of normal cells	8,277.33	2,269.83	4,986.67	10,648.89
Numerical density of TUNEL-positive cells	10.67	14.61	0.00	26.67
LI of TUNEL-positive cells	0.18	0.25	0.00	0.53
GA 16–19 weeks				
Numerical density of total cells	6,292.22	2,049.83	3,617.78	9,164.44
Numerical density of normal cells	6,236.67	2,043.10	3,573.33	9,120.00
Numerical density of TUNEL-positive cells	55.55	27.60	8.89	97.78
LI of TUNEL-positive cells	0.93	0.47	0.16	1.59
GA 20–23 weeks				
Numerical density of total cells	5,769.63	2,074.27	2,808.89	9,013.33
Numerical density of normal cells	5,696.30	2,074.55	2,711.11	8,871.11
Numerical density of TUNEL-positive cells	73.33	37.74	8.89	142.22
LI of TUNEL-positive cells	1.52	1.04	0.13	3.48
GA 24–27 weeks				
Numerical density of total cells	3,762.22	1,387.36	1,857.78	5,768.89
Numerical density of normal cells	3,664.45	1,352.02	1,777.78	5,626.67
Numerical density of TUNEL-positive cells	97.78	44.06	44.44	151.11
LI of TUNEL-positive cells	2.67	0.91	1.29	4.31
GA 28–31 weeks				
Numerical density of total cells	1,564.45	1,206.80	711.11	2,417.78
Numerical density of normal cells	1,524.45	1,225.65	657.78	2,391.11
Numerical density of TUNEL-positive cells	40.00	18.85	26.67	53.33
LI of TUNEL-positive cells	4.30	4.53	1.10	7.50
GA 32–40 weeks				
Numerical density of total cells	832.00	267.53	613.33	1,137.78
Numerical density of normal cells	792.89	243.14	613.33	1,093.33
Numerical density of TUNEL-positive cells	39.11	44.71	.00	115.56
LI of TUNEL-positive cells	4.27	3.92	0.00	10.16
Putamen				
GA 12–15 weeks				
Numerical density of total cells	6,680.00	2,903.69	4,293.33	10,906.67
Numerical density of normal cells	6,671.11	2,910.15	4,275.56	10,906.67
Numerical density of TUNEL-positive cells	8.89	10.27	.00	17.78
LI of TUNEL-positive cells	0.18	0.21	0.00	0.41
GA 16–19 weeks				
Numerical density of total cells	4,450.37	1,738.85	2,213.33	6,844.44
Numerical density of normal cells	4,389.6	1,738.60	2,133.33	6,791.11
Numerical density of TUNEL-positive cells	60.74	20.59	26.67	80.00
LI of TUNEL-positive cells	1.61	1.06	0.71	3.61
GA 20–23 weeks				
Numerical density of total cells	3,710.62	1,218.33	2,008.89	5,591.11
Numerical density of normal cells	3,639.51	1,204.03	1,946.67	5,502.22
Numerical density of TUNEL-positive cells	71.11	32.96	17.78	115.56
LI of TUNEL-positive cells	2.00	0.98	0.51	3.24
GA 24–27 weeks				
Numerical density of total cells	2,863.49	1,191.60	2,035.56	5,413.33
Numerical density of normal cells	2,788.57	1,162.29	2,008.89	5,288.89
Numerical density of TUNEL-positive cells	74.92	36.60	26.67	124.44
LI of TUNEL-positive cells	2.59	0.78	1.31	3.95
GA 28–31 weeks				
Numerical density of total cells	1,031.12	842.24	435.56	1,626.67
Numerical density of normal cells	995.56	842.24	400.00	1,591.11
Numerical density of TUNEL-positive cells	35.56	0.00	35.56	35.56
LI of TUNEL-positive cells	5.18	4.22	2.19	8.16

Table 1 (continued)

	Mean	SD	Min	Max
GA 32–40 weeks				
Numerical density of total cells	716.44	379.19	480.00	1,377.78
Numerical density of normal cells	652.44	282.47	444.44	1,137.78
Numerical density of TUNEL-positive cells	64.00	99.66	0.00	240.00
LI of TUNEL-positive cells	6.33	6.84	.00	17.42
Globus pallidus				
GA 12–15 weeks				
No brains available				
GA 16–19 weeks				
Numerical density of total cells	773.33	107.65	702.22	933.33
Numerical density of normal cells	760.00	117.14	675.56	933.33
Numerical density of TUNEL-positive cells	13.34	11.48	0.00	26.67
LI of TUNEL-positive cells	1.86	1.63	0.00	3.80
GA 20–23 weeks				
Numerical density of total cells	924.44	345.35	640.00	1,511.11
Numerical density of normal cells	908.44	338.91	631.11	1,484.44
Numerical density of TUNEL-positive cells	16.00	9.74	8.89	26.67
LI of TUNEL-positive cells	1.71	0.86	0.97	3.16
GA 24–27 weeks				
Numerical density of total cells	1,015.56	314.39	773.33	1,475.56
Numerical density of normal cells	957.78	268.47	746.67	1,351.11
Numerical density of TUNEL-positive cells	57.78	48.41	17.78	124.44
LI of TUNEL-positive cells	5.13	2.91	2.04	8.43
GA 28–31 weeks				
Numerical density of total cells	435.56	–	435.5	435.56
Numerical density of normal cells	346.67	–	346.67	346.67
Numerical density of TUNEL-positive cells	88.89	–	88.89	88.89
LI of TUNEL-positive cells	20.41	–	20.41	20.41
GA 32–40 weeks				
Numerical density of total cells	536.30	220.85	400.00	791.11
Numerical density of normal cells	509.63	206.05	373.33	746.67
Numerical density of TUNEL-positive cells	26.67	17.78	8.89	44.44
LI of TUNEL-positive cells	4.81	2.38	2.13	6.67

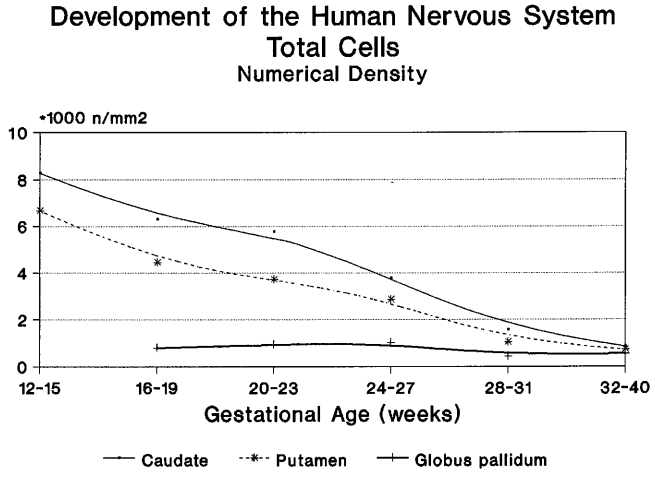

Fig. 3 Changes of the numerical density of all cells in the caudate nucleus, putamen, and globus pallidus with increasing gestational age

Table 2 Correlation coefficients of the evaluated parameters in the basal ganglia with age

Caudate nucleus	
Numerical density of total cells	–0.81**
Numerical density of normal cells	–0.81**
Numerical density of TUNEL-positive cells	0.03
LI of TUNEL-positive cells	0.57**
Putamen	
Numerical density of total cells	–0.76**
Numerical density of normal cells	–0.76**
Numerical density of TUNEL-positive cells	0.08
LI of TUNEL-positive cells	0.51**
Globus pallidus	
Numerical density of total cells	–0.44
Numerical density of normal cells	–0.48
Numerical density of TUNEL-positive cells	0.20
LI of TUNEL-positive cells	0.40

*P<0.01; **P<0.001

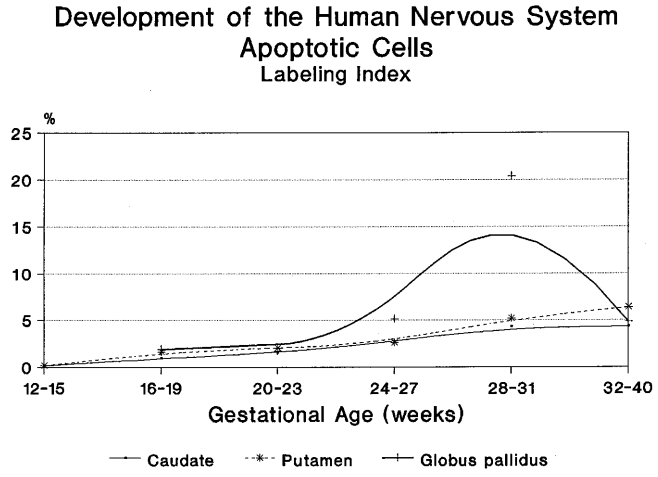

Fig. 4 Changes of the labeling index of TUNEL-labeled cells in the caudate nucleus, putamen, and globus pallidus with increasing gestational age

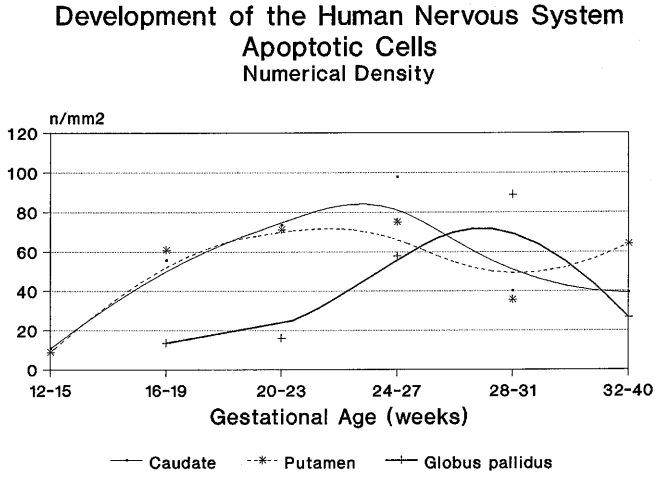

Fig. 5 Changes of the numerical density of TUNEL-labeled apoptotic cells in the caudate nucleus, putamen, and globus pallidus with increasing gestational age

positive TUNEL-assay reaction should not be considered as a specific marker of apoptosis but can also indicate necrotic cell death. Therefore, in the present investigation all TUNEL-positive cells showing histological features of necrosis were excluded [10]. Their number was exceedingly low, as could be expected in the developing brain [10]. Artifacts due to postmortem delay (i.e., clustering of stained cells as described for the in situ end-labeling assay in brain tissue of mice by [38]) were not encountered in the specimens of the present study, since only material with a postmortem delay of 24 h was used. Kingsbury et al. [25] suggested that DNA fragmentation in the human substantia nigra is influenced by antemortem hypoxia, pH of the investigated tissue and other perimortem markers for agonal status. Controlling and standardizing these factors for analyses of human brain tissue represents a desirable goal, which, however, in daily practice can never be reached.

In the dorsal striatum, i.e., the complex of the caudate nucleus and putamen, the numerical density of all cells was significantly decreased, whereas the labeling index of TUNEL-labeled cells was significantly increased with increasing gestational age. The results suggest that apoptosis in the striatum is at least one mechanism involved in the regulation of cell numbers during the embryonic development. It has previously been reported that cell density can be down-regulated by bcl-2 expression, an anti-apoptotic proto-oncogene. Down-regulated bcl-2 protein in high cell density might cause more apoptosis, resulting in cell elimination of overproduced cells [1, 15, 16, 22, 26, 36]. One triggering factor of apoptosis might be a high density of stem cells in the developing striatum. Morphologically, the striatum shows maturation of large neurons at weeks 28–30 of GA and of small neurons at weeks 33–36 of GA. Apoptosis in the striatum begins before neuronal maturation and continues during all stages of striatal maturation. The dorsal striatum forms afferent connections with the substantia nigra pars compacta, dorsal raphe nucleus, medial reticular formation, thalamus, subthalamic nucleus, and neocortex, and sends efferent connections to the globus pallidus and substantia nigra pars reticulata. Apoptotic cell death might occur as a consequence of the need to eliminate neurons that have failed to make appropriate synaptic connections. Most efferent connection sites, i.e., the globus pallidus and brain stem nuclei are already well developed by the second half of gestation. Maturation of neurons in the neocortex begins to mature in the deep pyramidal layer around the 24th week and continues throughout the fetal period. Apoptotic cell death in the striatum might occur closely related to the establishment of the efferent connections at first, and probably influences further the maturation of the afferent site such as the neocortex.

In the globus pallidus, apoptotic cells were observed during the 18th week of GA and their density was increased between weeks 20–23 and weeks 28–31, and decreased after week 32. The decrease of cell number and the increase of the LI did not reach the level of statistical significance. The pallidal neurons mature by the 24th week. The peak of apoptosis was observed after pallidal neuronal maturation. It is not known why the peak of apoptosis was observed about 4 weeks later than that of the striatum. The dorsal pallidum sends efferent fibers to the thalamus, subthalamic nuclei, and tegmental pedunculopontocerebellar nucleus and receives afferent fibers mainly from the striatum as well as from the subthalamic nucleus and the tegmental pedunculopontocerebellar nucleus. Between the 7th and 11th week of GA, most thalamic nuclear groups which form the main efferent regions of pallidal neurons have been established and the large neurons begin to acquire cytoplasmic bodies by week 24. Apoptosis in the globus pallidus might not only be responsible for the elimination of overproduced stem cells but occur in a more complicated form which is related not only to the maturation of afferent and efferent brain regions but also to other functions.

Thus, the establishment of neuronal connections might have a significant feedback on the amount of dying neurons. On the other hand, it is possible that the process of neuronal cell death is initiated at a certain period after the generation and maturation of neurons began and is independent of the creation of connections. Bayer et al. [3] generated neurogenetic timetables for the development of the basal ganglia based on long-survival [^{3}H]thymidine autoradiography in the rat and the estimated time of development in human. The age matches were based on correlations between the gross appearance of the forebrain and on similarities in the histological sections. Following their data, neurons are generated in the globus pallidus from embryonic day (E) 13 until E15 in the rat. In humans, they are generated from early in week 4 to the middle of week 6, migrate soon thereafter, and settle during early in week 7. In the caudoputamen complex neurons are generated from E16 until E20 in rats, while in humans neurons are generated from weeks 5 to 18. This delay in generation and maturation of neurons between the globus pallidus and the caudoputamen complex is also reflected in the data of the present report by the different begin of apoptosis in the human globus pallidus as compared to the caudate nucleus and the putamen.

Furthermore, the postnatal changes of apoptosis in basal ganglia are of interest. Waters et al. [42] reported that apoptotic cell death observed in the neonatal rat globus pallidus was greatest at day 1 and declined thereafter, such that negligible amounts of apoptotic cell death were detected at day 7 and none could be detected in the globus pallidus of adult animals. It was suggested that the apoptotic cell death in the neonatal globus pallidus might result from a temporary structure, which was subsequently redundant, rather than the necessary elimination of neurons that failed to make appropriate synaptic connections. Apoptotic cells in the caudate nucleus tended to form clusters of several cells. This process has been described in the apoptotic cell death of the neonatal rat globus pallidus and it was suspected that this grouping was the preprogrammed death of sister cells born at the same time [42].

In conclusion, the data of the present study show that apoptotic cell death was observed in the basal ganglia of the developing human brain. It is suggested that apoptosis might be one mechanism involved in the regulation of cell numbers by deletion of overproduced stem cells; however, the triggering factors and functions of apoptosis might be heterogeneous. Further molecular biological studies on intracellular molecules such as the proto-oncogenes, APO-1/FAS, c-myc, bcl-2, ICE families will be necessary for elucidating other possible mechanisms resulting in cell death.

Acknowledgments The authors thank Ms. Irene Kiss and Angela Henn for their skillful technical assistance. The help of Ida C. Llenos, MD, in correcting the manuscript is highly appreciated.

References

1. Allsopp TE, Wyatt S, Paterson HF, Davies AM (1993) The proto-oncogene bcl-2 can selectively rescue neurotrophic factor-dependent neurons from apoptosis. Cell 73: 295–307
2. Ashwell K (1990) Microglia and cell death in the developing mouse cerebellum. Dev Brain Res 55: 219–230
3. Bayer SA, Altman J, Russo RJ, Zhang X (1995) Embryology. In: Duckett S (ed) Pediatric neuropathology. Williams & Wilkins, Baltimore, pp 54–107
4. Buttyan R, Olsson CA, Pintar J (1989) Induction of TRPM-2 gene in cells undergoing programmed cell death. Mol Cell Biol 9: 3473–3481
5. Charriaut-Marlangue C, Ben-Ari Y (1995) A cautionary note on the use of the TUNEL stain to determine apoptosis. NeuroReport 7: 61–64
6. Chu-Wang IW, Oppenheimer RW (1978) Cell death of motor neurons in the chick embryo spinal cord-1. A light and electron microscopic study of naturally occurring and induced cell loss during development. J Comp Neurol 177: 33–58
7. Clarke PGH (1985) Neuronal death during development in the isthmo-optic nucleus of the chick, sustaining role of afferents from the tectum. J Comp Neurol 234: 365–379
8. Clarke PGH (1985) Neuronal death in the development of the vertebrate nervous system. Trends Neurosci 8: 345–349
9. Clarke PGH (1990) Developmental cell death: morphological diversity and multiple mechanisms. Anat Embryol (Berl) 181: 195–213
10. Clarke PGH (1999) Apoptosis versus necrosis. How valid a dichotomy for neurons? In: Koliatsos VE, Ratan RR (eds) Cell death and diseases of the nervous System. Humana Press, New Jersey, pp 3–28
11. Cowan WM, Fawcett JW, O'Leary DDM, Stanfield BB (1984) Regressive events in neurogenesis. Science 225: 1258–1265
12. Decker RS (1974) Lysosomal packaging in differentiating and degenerating lateral motor column neurons. J Cell Biol 61: 599–612
13. Evan GI, Wyllie AH, Gilbert CS (1992) Induction of apoptosis in fibroblasts by c-myc protein. Cell 69: 119–128
14. Ferrer I, Soriano E, Del Rio JA, Alcantara S, Auladell C (1992) Cell death and removal in the cerebral cortex during development. Prog Neurobiol 39: 1–43
15. Ferrer I, Tortosa A, Blanco R (1994) Naturally occurring cell death in the developing cerebral cortex of the rat. Evidence of apoptosis-associated internucleosomal DNA fragmentation. Neurosci Lett 182: 77–79
16. Garcia I, Martinou I, Tsujimoto Y, Martinou JC (1992) Prevention of programmed cell death of sympathetic neurons by the bcl-2 proto-oncogene. Science 258: 302–305
17. Gould E, McEwen BS (1993) Neuronal birth and death. Curr Opin Neurobiol 3: 676–682
18. Gundersen HJG (1977) Notes on the estimation of the numerical density of arbitrary profiles: the edge effects. J Microsc 111: 219–223
19. Hamburger V, Oppenheim RW (1982) Naturally occurring neuronal death in vertebrates. Neurosci Comment 1: 38–55
20. Janec E, Burke RE (1993) Naturally occurring cell death during postnatal development of the substantia nigra pars compacta of rat. Mol Cell Neurosci 4: 30–35
21. Janowsky JS, Findlay BL (1983) Cell degeneration in early development of the forebrain and cerebellum. Anat Embryol (Berl) 167: 439–447
22. Kane DC, Sarafian TA, Anton R (1993) Bcl-2 inhibition of neural death: decreased generation of reactive oxygen species. Science 262: 1274–1277
23. Keino H, Masaki S, Kawarada Y, Naruse I (1994) Apoptotic degeneration in the arhinencephalic brain of the mouse mutant Pdn/Pdn. Dev Brain Res 78: 161–168
24. Kerr JFR, Wyllie AH, Currie AR (1972) Apoptosis: a basic biological phenomenon with wide ranging implications in tissue kinetics. Br J Cancer 26: 239–257

25. Kingsbury AE, Marsden CD, Foster OJ (1998) DNA fragmentation in human substantia nigra: apoptosis or perimortem effect? Mov Disord 13: 877–884
26. LeBrun DP, Warnke RA, Cleary ML (1993) Expression of bcl-2 in fetal tissue suggests a role of morphogenesis. Am J Pathol 142: 743–753
27. Levi-Montalcini R (1987) The nerve growth factor-35 years later. EMBO J 6: 1145–1154
28. Lowe S, Jacks T, Housman DE, Ruley RE (1994) Abrogation of oncogene-associated apoptosis allows transformation of p53-deficient cells. Proc Natl Acad Sci USA 91: 2026–2030
29. Matsuyama T, Hata R, Tagaya M (1994) Fas antigen mRNA induction in postischemic murine brain. Brain Res 657: 342–346
30. Migheli A, Cavalla P, Marino S, Schiffer D (1994) A study of apoptosis in normal and pathologic nervous tissue after in situ end-labeling of DNA strand breaks. J Neuropathol Exp Neurol 53: 606–616
31. Miura M, Zhu H, Rotello R, Hartweieg EA, Yuan J (1993) Induction of apoptosis in fibroblasts by IL-1β (β-converting enzyme, a mammalian homolog of the *C. elegans* cell death gene ced-3. Cell 75: 653–660
32. Naruse I, Keino H (1991) Apoptosis in the developing CNS. Prog Neurobiol 47: 135–155
33. Oppenheim RW (1991) Cell death during development of the nervous system. Annu Rev Neurosci 14: 453–501
34. Pilar G, Landmesser L (1976) Ultrastructural differences between embryonic cell death in normal and peripherally deprived ciliary ganglia. J Cell Biol 68: 339–356
35. Raff MC, Barres BA, Burne JF, Coles HF, Ishizaki Y, Jacobson MD (1993) Programmed cell death and the control of cell survival: lessons from the nervous system. Science 262: 695–700
36. Reed JC (1994) Bcl-2 and the regulation of programmed cell death. J Cell Biol 124: 1–6
37. Saunders JW (1996) Death in embryonic organs. Science 154: 604–612
38. Schallock K, Schulz-Schaeffer WJ, Giese A, Kretzschmar HA (1997) Postmortem delay and temperature conditions affect the in situ end-labeling (ISEL) assay in brain tissue of mice. Clin Neuropathol 16: 133–136
39. Schwartz LM, Smith SW, Jones ME, Osborne BA (1993) Do all programmed cell deaths occur via apoptosis? Proc Natl Acad Sci USA 90: 980–984
40. Smeyne R, Vendrell M, Hatward M (1993) Continuous c-fos expression precedes programmed cell death in vivo. Nature 363: 166–169
41. Waite PME, Lixin L, Ashwell KWS (1992) Development and lesion induced cell death in the rat ventrobasal complex. NeuroReport 3: 485–488
42. Waters CM, Moser W, Walkinshaw G, Mitchell IJ (1994) Death of neurons in the neonatal rodent and primate globus pallidus occurs by a mechanism of apoptosis. Neuroscience 63: 881–894
43. Weis S (1991) Morphometry in the Neurosciences. In: Wenger E, Dimitrov L (eds) Digital image processing and computer graphics. Theory and application. Oldenbourg, Wien, pp 306–326
44. Wyllie AH, Morris RG, Smith AL, Dunlop D (1984) Chromatin cleavage in apoptosis: association with condensed chromatin morphology and dependence on macromolecular synthesis. J Pathol 142: 67–78
45. Zakeri Z, Bursch W, Tenniswood M, Lockshin RA (1995) Cell death: programmed, apoptosis, necrosis, or other? Cell Death Differ 2: 87–96